frontiers | Frontiers in Physics

TYPE Original Research
PUBLISHED 20 November 2024
DOI 10.3389/fphy.2024.1502544

OPEN ACCESS

EDITED BY
Shuo Liu,
Hebei University of Technology, China

REVIEWED BY
Yudong Lian,
Hebei University of Technology, China
Hongli Wang,
North University of China, China
Bin Yin,
Ocean University of China, China

*CORRESPONDENCE
Zhiyong Wang,
zhaoguanrui@emails.bjut.edu.cn

RECEIVED 27 September 2024
ACCEPTED 07 November 2024
PUBLISHED 20 November 2024

CITATION
Yin Y, Ge T, Li G, Xue C and Wang Z (2024) Effect of fiber twist angle and non-uniform symmetric alignment on signal combiner. *Front. Phys.* 12:1502544. doi: 10.3389/fphy.2024.1502544

Effect of fiber twist angle and non-uniform symmetric alignment on signal combiner

Yuyi Yin, Tingwu Ge, Guanzheng Li, Chuang Xue and Zhiyong Wang*

Institute of Laser Engineering, Beijing University of Technology, Beijing, China

Signal beam combiners play a pivotal role in enhancing the output power of fiber lasers, which have wide-ranging applications from industrial processing to medical and military uses. This paper explores the influence of fiber twist angle and non-uniform symmetric arrangement on the performance of 19 × 1 fiber signal combiners. A simulation model was developed to analyze the impact of these parameters under adiabatic tapering conditions and the principle of brightness conservation. The model allowed for a systematic investigation of how varying twist angles and non-uniform spacings affect the combiner's performance metrics, such as transmission efficiency and beam quality. The study found that an optimal balance between high transmission efficiency (up to 98.5%) and good beam quality (minimum M^2 factor of 1.06) can be achieved when the twist angle is kept below 60° and the non-uniform spacing is maintained within 10–30 μm. These conditions ensure minimal degradation of the beam quality while maximizing the transmission efficiency of the combiner. These findings offer valuable insights into the optimization of signal combiner design, which is critical for advancing high-power fiber laser systems. By carefully controlling the fiber twist angle and non-uniform spacing, designers can achieve superior performance in fiber laser applications, thereby enhancing the overall efficiency and reliability of these systems. This research contributes to the broader field of optical engineering by providing a deeper understanding of the underlying principles that govern the performance of signal combiners.

KEYWORDS

signal combiner, torsion, non-uniform symmetric alignment, transmission efficiency, beam quality

1 Introduction

Fiber lasers, known for their high efficiency, excellent beam quality, and modular design, are widely used in industrial processing, medical surgery, and military applications. However, the output power of a single fiber laser is limited by the physical and optical properties of the fiber. Signal combiners address this limitation by merging multiple low-power fiber lasers into a single, high-power output, thereby expanding the application range and performance capabilities of fiber lasers [1–4].

Signal combiners play a crucial role in modern optics and communication technology, as they not only increase the output power but also enhance the overall efficiency, reliability, and signal stability of fiber laser systems [5–7]. Despite their importance, practical implementation faces technical challenges, particularly with respect to fiber twisting angles and non-uniform symmetrical arrangements during the tapering process. Tapering, a

critical step in combiner manufacturing, involves controlled stretching of fibers to achieve efficient signal merging [8]. The twisting and non-uniformity that occur during this process can significantly affect the transmission efficiency and beam quality of the combiner, making precise control of these parameters crucial for optimal performance [9, 10].

Currently, signal combiners are a focal point of scholarly attention, especially in signal combiner fabrication, high-power all-fiber coherent synthesis, signal combiner design, and laser combiner performance evaluation. For example, [11] successfully manufactured a 7 × 1 mid-infrared fiber combiner using advanced low-temperature fusion tapering technology [11]. The research results demonstrate that the combiner exhibits outstanding fusion quality with minimal losses at fusion points (only 0.45 dB), and can withstand a tension force exceeding 300g, achieving an average transmission efficiency of approximately 80% and the highest output power of 4.32W in a single channel, showcasing its exceptional transmission characteristics and high-power tolerance. [12] developed a special (6 + 1) × 1 reverse pump/signal combiner, with both input and output ends using 50 μm large core diameter signal fibers [12]. Through feedback calibration of the M^2 beam quality evaluation factor, a combiner was successfully developed to maintain high beam quality, with a beam quality degradation ratio of only 3.4%. This device was applied in a simple MOPA structure narrow linewidth laser system, achieving a near single-mode output of 4.1 kW and a Raman suppression ratio of 40.5 dB, demonstrating its potential in high-performance laser systems.

Despite the abundant research on signal combiners, there is relatively little focus on the specific parameters of fiber twisting angles and non-uniform symmetrical arrangements, which represents a current research gap [13–16]. This paper investigates the impact of fiber twisting angles and non-uniform symmetrical arrangements on signal combiners. The study delves into the effects of these parameters during the tapering process on the performance of the combiner, comparing the transmission efficiency and beam quality under different conditions to determine the optimal twisting angles and non-uniform arrangements. The goal is to optimize the design of fiber signal combiners and provide important technical support for increasing the output power and performance of fiber lasers.

2 Theoretical basis

2.1 Beam propagation method

In 1978, Fleck et al. first proposed the Beam Propagation Method (BPM), which accurately solves the Helmholtz equation to obtain the mode field distribution of different parts of the optical fiber. This calculation method has significant implications in the field of optical waveguides, as it can simulate the propagation characteristics of the mode field within them, providing a powerful mathematical tool for research in optical fiber communication and related technologies [17].

BPM is crucial for calculating the coupling efficiency between the input fibers and the output fiber, which directly impacts the overall transmission efficiency. By simulating the mode field distribution and the overlap integral, BPM helps in visualizing and analyzing how light modes evolve through the tapered region, identifying any modal instabilities or distortions that could degrade beam quality. The method also allows for the optimization of design parameters such as the twist angle and the non-uniform symmetric arrangement distance. For instance, the simulations show that maintaining a twist angle not exceeding 60° and a non-uniform symmetric arrangement distance between 10 and 30 μm leads to high transmission efficiency (up to 98.5%) and better beam quality (minimum M^2 factor of 1.06).

Furthermore, BPM provides a robust theoretical framework for validating the simulation results, ensuring that the performance metrics, such as transmission efficiency and beam quality, are based on a well-validated physical model. This enhances the credibility of the findings and supports the practical applicability of the optimized design. By leveraging BPM, the manuscript offers a solid theoretical foundation for the design and optimization of the 19 × 1 fiber signal combiner, contributing to the development of more efficient and reliable high-power fiber laser systems [18–21].

Based on the Maxwell's equations, we can delve into the fundamental properties of light propagation within optical fibers shown as Equations 1–4 [22]:

$$\nabla \times H = J + \frac{\partial D}{\partial t} \tag{1}$$

$$\nabla \times E = -\frac{\partial B}{\partial t} \tag{2}$$

$$\nabla \bullet D = \rho \tag{3}$$

$$\nabla \bullet B = 0 \tag{4}$$

To determine the electric field strength E, electric displacement vector D, magnetic induction intensity B, and magnetic field strength H, it is necessary to relate them to material equations. The characteristics of material equations are deeply influenced by the medium in which the electromagnetic fields exist shown as Equations 5, 6 [23]:

$$D(r) = \varepsilon(r) \bullet E(r) \tag{5}$$

$$B(r) = \mu(r) \bullet H(r) \tag{6}$$

based on this, the wave equation for optical fibers (where ε is a constant, $\nabla\varepsilon = 0$) can be further derived:

$$\nabla^2 E + k^2 E = 0 \tag{7}$$

$$\nabla^2 H + k^2 H = 0 \tag{8}$$

Equations 7, 8 represent the vector Helmholtz equation. In this coordinate system, the x, y, and z components of E and H strictly follow the laws of the scalar Helmholtz equation:

$$\nabla^2 \psi + k^2 \psi = 0 \tag{9}$$

In the Equation 9, ψ represents the components of E or H.

2.2 Conical fiber characteristics

The tapered fiber in the signal combiner is made of fiber through a special fusion stretching process, which changes the diameter and shape of the fiber, thus affecting its optical properties.

2.2.1 Adiabatic tapering condition

Adiabatic tapering is used to describe the extremely small degree of change in the diameter of the taper zone after the fiber is processed by the tapering process. This characteristic ensures that when light propagates inside the tapered fiber, it can be tightly confined to the core area, effectively preventing light from leaking to the outer cladding [24]. That is:

$$\frac{\Delta r}{r} = 1 \tag{10}$$

In the formula, $=r$ represents the difference in the diameter of the fiber end face before and after the tapering process, while λ represents the original size parameters of the fiber. If the rate of change of the core diameter is too large, the propagation mode of the light wave will transition from the fundamental mode state to a higher-order mode, leading to a coupling phenomenon in the fiber. Usually, the propagation constant β is used to quantitatively describe the transmission mode in the fiber [25], defined as follows Equation 11:

$$\beta = \frac{2\pi}{\lambda} n_{\text{eff}} \tag{11}$$

In the formula, n_{eff} represents the effective refractive index of the fiber, while λ represents the transmission wavelength. In the definition of the fiber transmission mode, the propagation constant of the fundamental mode is denoted as β_1 , and the propagation constant of the higher-order mode is denoted as β_2. Based on this, the beat length of the fiber is precisely defined as Equation 12:

$$L_B = \frac{2\pi}{\beta_1 - \beta_2} \tag{12}$$

Expressing the change in core diameter in terms of beat length:

$$\Delta r = L_B \frac{dr}{dz} \tag{13}$$

Substituting Equation 13 into Equation 10, we get Equation 14:

$$\frac{dr}{dz} \le \frac{r}{L_B} \tag{14}$$

When the first high-order mode propagation constant is taken as β_2 , the value L_B reaches a maximum, and at this point, the adiabatic tapering standard is most stringent. It can be inferred that under this standard, the transmission loss of the fiber will be minimized. The tapering process of the fiber is usually considered as linear tapering, that is, the slope of the fiber diameter remains constant over the entire taper zone. Therefore, for the entire taper zone $dz = L, dr = r_1 - r_2$, the initial diameter of the fiber is set as r_1, and the waist diameter formed after tapering is r_2 . Further defining the taper ratio of the fiber $TR = r_1/r_2$, the adiabatic tapering condition of the fiber can be expressed as Equation 15 [26]:

$$L \ge (TR - 1)L_B \tag{15}$$

From Equation 15, it is evident that a longer fiber taper zone better satisfies the adiabatic tapering condition, reducing losses during the tapering process. However, in practical applications, an overly long taper zone can increase the fragility of the fiber and complicate packaging. Therefore, it is necessary to balance the theoretical benefits of adiabatic tapering with practical considerations. This involves determining an optimal taper zone length that minimizes losses while ensuring the fiber's stability and ease of packaging.

2.2.2 Brightness conservation principle

In the coupling process from input fiber to output fiber of the laser, the brightness conservation principle plays an important role. This principle elaborates from the perspective of the fiber's reception and emission capabilities towards the laser, delving into the necessary conditions for achieving efficient coupling between lasers and fibers.

During the coupling process between laser and fiber, the reception and emission capabilities of the fiber can be quantitatively expressed through the parameter of Integrated Brightness (IB) [27]. When the laser is uniformly incident on the fiber, the integrated brightness can be specifically described as Equation 16:

$$IB = AR\int_0^{\Omega_\phi} d\Omega \propto A\int_0^{\phi} \sin\varphi d\varphi = A[1 - \cos\phi] \tag{16}$$

Where A represents the irradiation area of the fiber, R is the distribution profile of irradiance, and ϕ denotes the laser acceptance angle of the fiber. There exists a proportional relationship between the numerical aperture NA of the fiber and sin ϕ. Due to the small acceptance angle of the fiber under normal circumstances, it can be derived that sin $\phi \approx \phi$. In this scenario, integrated brightness can be expressed as Equation 17:

$$IB \propto A[1 - \cos\phi] \approx \frac{A}{2} NA^2 \tag{17}$$

The concept of Brightness Ratio (BR) is introduced to quantify the relative relationship of integrated brightness between input and output fibers [28]. Its mathematical expression is as follows Equation 18:

$$BR = \frac{IB_{\text{out}}}{IB_{\text{in}}} = \frac{D_{\text{out}}^2\left[1 - \cos\phi_{\text{out}}\right]}{nD_{\text{in}}^2\left[1 - \cos\phi_{\text{in}}\right]} = \frac{D_{\text{out}}^2 NA_{\text{out}}^2}{nD_{\text{in}}^2 NA_{\text{in}}^2} \tag{18}$$

In the application of signal combiners, D_{in} and NA_{in} respectively represent the diameter and numerical aperture of the input fiber bundle layer after tapering, while D_{out} 、 NA_{out} refers to the diameter and numerical aperture of the output fiber core. n indicates the number of input fibers received by the combiner. IB_{in} and IB_{out} as parameters, respectively measure the reception and emission capabilities of the input fiber bundle layer and the output fiber core in terms of light. When $BR \ge 1$ is satisfied, i.e., when the reception capability of the output fiber exceeds the emission capability of the input fiber, the light intensity in the input fiber can be completely coupled to the output fiber, thereby achieving a low-loss coupling process.

Based on the brightness conservation principle, to ensure efficient transmission of the signal combiner, the output fiber should have a larger core diameter and numerical aperture. However, improving the beam quality of the output laser requires reducing

the number of modes excited during fusion splicing. Therefore, when selecting the size of the output fiber core, it is necessary to balance transmission efficiency and beam quality in order to achieve the relative optimization of the performance indicators of the signal combiner.

2.3 Signal combiner quality metrics

The quality metrics of the signal combiner mainly focus on its performance and reliability, which are crucial for evaluating and ensuring that the combiner meets specific application requirements. This paper primarily adopts the M^2 factor and transmission efficiency as the quality metrics for the signal combiner.

2.3.1 M^2 factor

The M^2 factor is defined as the product of the actual beam's spot size and the far-field divergence angle, divided by the product of the spot size and the far-field divergence angle corresponding to the ideal fundamental Gaussian beam.

It is determined through the second moment [29] to ascertain the waist radius of the optical fiber [13]:

$$\overline{x} = \frac{\int_{-\infty}^{\infty}\int_{-\infty}^{\infty} x \cdot E(x,y) \cdot E^*(x,y)dxdy}{\int_{-\infty}^{\infty}\int_{-\infty}^{\infty} E(x,y) \cdot E^*(x,y)dxdy} \tag{19}$$

$$\omega_x = 2\sqrt{\frac{\iint (x-\overline{x})^2 E(x,y) \cdot E^*(x,y)dxdy}{\iint E(x,y) \cdot E^*(x,y)dxdy}} \tag{20}$$

$$\overline{y} = \frac{\int_{-\infty}^{\infty}\int_{-\infty}^{\infty} y \cdot E(x,y) \cdot E^*(x,y)dxdy}{\int_{-\infty}^{\infty}\int_{-\infty}^{\infty} E(x,y) \cdot E^*(x,y)dxdy} \tag{21}$$

$$\omega_y = 2\sqrt{\frac{\iint (y-\overline{y})^2 E(x,y) \cdot E^*(x,y)dxdy}{\iint E(x,y) \cdot E^*(x,y)dxdy}} \tag{22}$$

In the formula: $(\overline{x},\overline{y})$ represents the centroid coordinates of the electric field, $E(x,y)$ represents the electric field distribution function, and ω_x and ω_y represent the second-order moment widths of the electric field in the x and y directions, respectively shown as Equations 19–22.

According to the definition of the M^2 factor, we can obtain [30]:

$$M_x^2 = \lim_{z\to\infty} \frac{\pi\omega_x(0)\omega_x(z)}{z\lambda} = \pi\omega_x\Theta_z n \tag{23}$$

$$M_y^2 = \lim_{z\to\infty} \frac{\pi\omega_y(0)\omega_y(z)}{z\lambda} = \pi\omega_y\Theta_n \tag{24}$$

$$M^2 = \sqrt{M_x^2 \cdot M_y^2} \tag{25}$$

M_x^2 and M_y^2 respectively represent the M^2 factor in the x and y directions, while Θ_z and Θ_n respectively represent the effective beam radius of the laser in the far field in the x and y directions. z and n represent the coordinates in the far-field plane shown as Equations 23–25.

The laser output from the fiber is a mixture of the fundamental Gaussian beam and higher-order mode Gaussian beams. Therefore, it is appropriate to evaluate beam quality with the ideal fundamental Gaussian beam as a reference. When the laser passes through an ideal optical system, the beam parameter product remains constant, making the M^2factor a constant quantity [31]. This characteristic enables the M^2 factor to rigorously and comprehensively reflect the beam quality of different fiber laser systems. As the M^2factor is referenced to the ideal fundamental Gaussian beam and considers both near-field and far-field characteristics of the beam, it is particularly suitable for evaluating the quality of signal combiners.

2.3.2 Transmission efficiency

Assuming that the mode field of the tapered input fiber bundle is defined as $E_{in}(x,y,z)$, when this mode field is coupled to the output fiber, its mode field representation can be viewed as a linear superposition of all excitable mode fields in the output fiber shown as Equation 26 [16]:

$$E(x,y,z) = \sum_{1}^{M}\sum_{1}^{N} C_{mn}E_{mn}(x,y,z) \tag{26}$$

In the equations, $E_{mn}(x,y,z)$ represents the (mn) th-order mode in the output fiber, i.e., one of the modes that can be excited in the fiber. The total number of excitable modes is denoted as $M \times N$ (where m,n are non-negative integers not greater than M, N, reflecting the mode capacity of the fiber. Meanwhile, C_{mn} represents the mode coefficient, which quantifies the proportion of each mode in all excitable modes. Its expression [32] is given by Equation 27:

$$C_{mn} = \sqrt{\alpha}_{mn} = \frac{\iint E_{in}(x,y,z) \times E_{mn}^*(x,y,z)dxdy}{\sqrt{\iint |E_{in}(x,y,z)|^2 dxdy \cdot \iint |E_{mn}(x,y,z)|^2 dxdy}} \tag{27}$$

Here, α_{mn} represents the ratio of the power of the (mn) th-order mode to the total input power.

Based on the proportion of power carried by each mode, the coupling efficiency at the fusion point can be calculated [33]:

$$T = \sum_{1}^{M}\sum_{1}^{N} \alpha_{mot} \tag{28}$$

From Equation 28, it can be observed that an increase in the number of excited modes during the coupling process will directly lead to an improvement in the coupling efficiency, thereby significantly enhancing the overall transmission efficiency of the signal combiner [34].

2.4 Theoretical background and practical application

Fiber signal combiners play a crucial role in high-power laser systems by merging multiple low-power fiber lasers into a single, high-power output. This technology is widely applied in industrial processing, medical surgery, and military applications due to its ability to significantly enhance the overall efficiency, reliability, and signal stability of fiber laser systems. However, current designs face limitations, such as reduced transmission efficiency and degraded

beam quality, which are primarily influenced by the physical properties of the fibers and the alignment during the tapering process. The twisting and non-uniformity that occur during this critical manufacturing step can severely impact the performance of the combiner.

To address these issues, the study focuses on optimizing the design of 19 × 1 fiber signal combiners by investigating the effects of fiber twist angle and non-uniform symmetric alignment. Specifically, the study explores how adjusting the twist angle and maintaining controlled non-uniform spacing can lead to significant improvements in both transmission efficiency and beam quality. By doing so, the aim is to overcome the existing limitations and provide a more robust solution for high-power fiber laser systems.

2.5 Model assumptions and simulation conditions

In developing the simulation model, adherence to fundamental principles of light propagation and the conservation of brightness ensures that the model accurately reflects the behavior of light within the fiber combiner. The simulation is conducted under adiabatic tapering conditions, where the gradual change in the fiber's cross-sectional area minimizes loss and distortion of the propagating signals. The model assumes an idealized environment but incorporates realistic parameters to closely mimic actual operating conditions.

For the simulations, a range of twist angles not exceeding 60° is specifically focused on, as higher angles tend to introduce excessive stress and deformation, leading to lower transmission efficiencies and poorer beam quality. Additionally, the non-uniform symmetric arrangement distance is maintained between 10 and 30 μm. This range is based on preliminary studies indicating that it optimally balances efficient signal combination with minimal interference. These parameter choices are grounded in a thorough understanding of the underlying physics and have been selected to represent a broad spectrum of potential real-world scenarios, thereby enhancing the applicability and relevance of the findings [35–38].

3 Methods

Building on the previous theoretical framework, this study constructs a basic simulation model of a fiber signal combiner to analyze the effects of fiber twisting angles and non-uniform asymmetric arrangements on the signal combiner [39].

In the established simulation model, the beam propagation method is employed to simulate the propagation of light waves in complex media. This method considers changes in refractive index, fiber structure, and the interaction between fibers. Based on the wave optics simulation of the propagation characteristics of light waves in the signal combiner, combined with the beam propagation method, the basic simulation model of a 19 × 1 fiber signal combiner is established using the Beam Prop module in the RSoft software package, as shown in Figure 1.

The 19 × 1 fiber signal combiner selected in this study represents a balanced solution, integrating practicality, efficiency, and the stringent demands of high-power laser systems. This

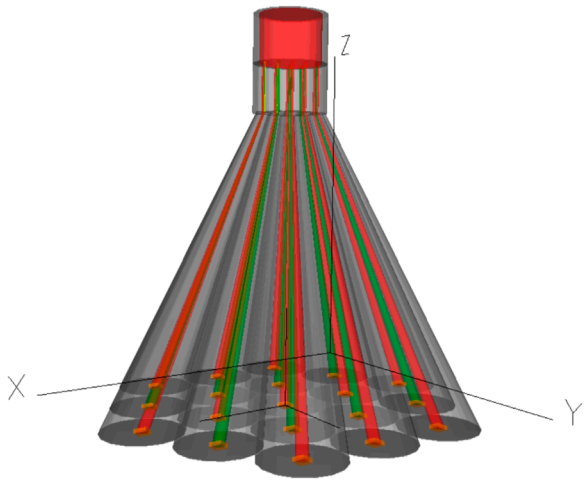

FIGURE 1
Simulation model of 19 × 1 fiber signal combiner.

design consolidates 19 low-power input fibers into a single, high-power output, significantly amplifying power while maintaining design and fabrication simplicity. The 19 × 1 configuration achieves impressive transmission efficiency (up to 98.5%) and maintains excellent beam quality ($M^2 \geq 1.06$), ensuring minimal loss and distortion. Leveraging standard optical fibers and established techniques, such as adiabatic tapering, it simplifies alignment and coupling, enhancing manufacturability. Moreover, its performance aligns with the specific needs of industrial, medical, and military applications, supporting tasks like cutting, welding, and precise material processing. The 19 × 1 combiner also provides scalability and adaptability, enabling parallel use or expansion to accommodate higher power requirements. By adopting the 19 × 1 fiber signal combiner, this research aims to optimize for both high performance and practical feasibility, addressing existing limitations and improving the reliability of fiber laser systems [40].

The simulation model for the fiber signal combiner employs 20/130 μm fibers as inputs and a 105/125 μm fiber for the output. The 20/130 μm fibers, featuring a 20 μm core diameter with a numerical aperture (NA) of 0.08 for the core and 0.46 for the cladding, are selected for their mode control and efficient light collection, critical for maintaining high beam quality and effective coupling. In contrast, the 105/125 μm output fiber, with a 105 μm core diameter and an NA of 0.22, is designed to manage higher power densities and reduce modal dispersion, ensuring a stable and robust output. This fiber combination ensures high transmission efficiency and excellent beam quality, with the smaller input fibers providing precise mode control and the larger output fiber offering mechanical durability and compatibility with existing optical systems.

During the adiabatic tapering process, the specified diameters enable controlled tapering, minimizing energy loss and preserving the integrity of the optical signal. This selection of fiber dimensions optimally balances efficient signal transmission, beam quality, and manufacturability, making it well-suited for high-power, high-quality laser applications.

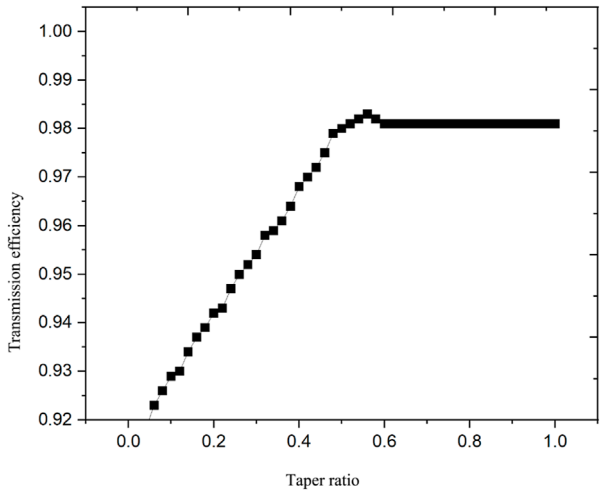

FIGURE 2
Transmission efficiency of signal combiner with different taper ratio.

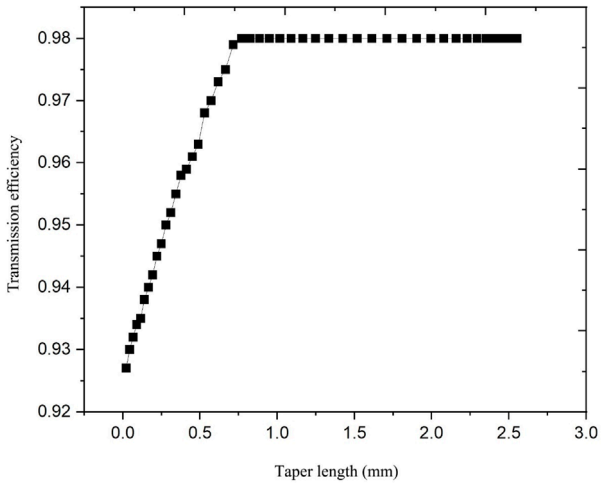

FIGURE 3
Transmission efficiency of signal combiner with different taper lengths.

4 Results and analysis

4.1 Impact of taper ratio and length on the signal combiner

Optimizing these parameters ensures an adiabatic process, minimizing energy loss and enhancing the beam quality. Simulation analysis is used to determine the optimal taper ratio and length, guiding the experimental production and reducing trial-and-error costs [41, 42]. Figure 2 illustrates the transmission efficiency of a single fiber signal combiner under different taper ratios, highlighting the importance of these parameters in achieving optimal performance.

From Figure 2, it can be observed that as the taper ratio increases, the transmission efficiency of a single fiber signal combiner gradually improves. When the taper ratio reaches 0.52, the transmission efficiency of a single fiber signal combiner reaches a peak and remains relatively stable. Therefore, the taper ratio for the signal combiner is set to 0.52.

Setting the taper ratio to 0.52, the transmission efficiency of a single fiber signal combiner under different taper lengths is shown in Figure 3.

As shown in Figure 3, the transmission efficiency of a single fiber signal combiner increases sharply as the taper length increases from 0 mm to 0.75 mm, and then stabilizes. At a taper length of about 1.01686 mm, the efficiency reaches a high and stable value. Thus, a 1 mm taper length is optimal, balancing efficiency and stability.

The ideal parameters for the combiner, based on simulations, are a 1 mm taper length and a 0.52 taper ratio, adhering to adiabatic tapering and brightness conservation principles. These settings yield an M^2 factor of 1.06 and a maximum transmission efficiency of 98.5%.

An M^2 factor of 1.06 indicates near-ideal beam quality, with minimal deviations. The 98.5% transmission efficiency demonstrates that the combiner effectively combines and transmits optical power with minimal loss.

Fiber bending also affects transmission; a 5 cm bending radius results in approximately 90% efficiency compared to a straight fiber. This slight difference does not significantly impact the overall simulation results.

In summary, the optimized design parameters—1 mm taper length, 0.52 taper ratio, M^2 of 1.06, and 98.5% efficiency—provide a solid foundation for the combiner's development and fabrication.

The length of the taper affects the adiabaticity of the mode evolution. A longer taper can ensure better adiabaticity, leading to higher transmission efficiency and potentially better beam quality. However, an excessively long taper may introduce additional losses due to increased interaction with the cladding and other factors.

The taper ratio, defined as the ratio of the final diameter to the initial diameter, influences the mode field distribution and coupling efficiency. An optimal taper ratio ensures that light modes are well-confined and efficiently transferred from the input fibers to the output fiber. A non-adiabatic taper can lead to mode mixing and increased beam divergence, negatively affecting the M^2 factor.

4.2 The impact of twist angle on the signal combiner

The twist angle of the optical fibers significantly impacts light propagation, mode distribution, and the overall performance of the beam combiner, including transmission efficiency and output beam quality. Moderate twisting reduces crosstalk between adjacent fibers by maintaining proper spacing and alignment, leading to better coupling and higher efficiency.

Based on the simulation model, various twist angles were analyzed to assess their effects on the signal combiner's performance, as shown in Figure 4. The results indicate that a moderate twist angle optimally balances fiber spacing and alignment, thereby enhancing the combiner's overall performance.

The transmission efficiency and beam quality of the signal combiner at different twist angles are shown in Figure 5.

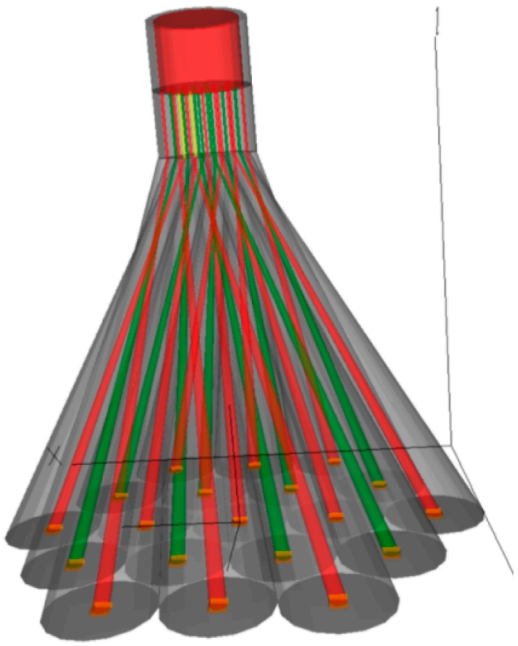

FIGURE 4
Schematic diagram of torsion angle change.

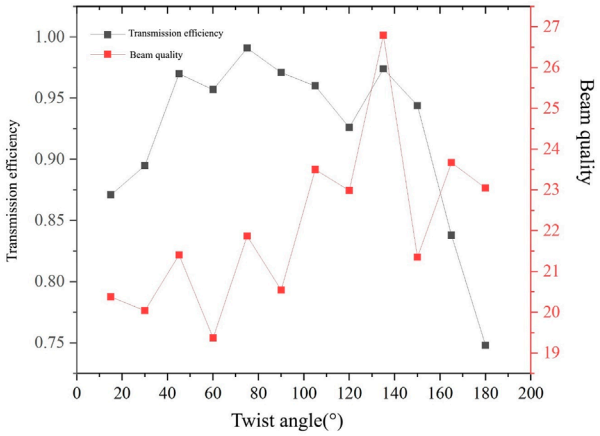

FIGURE 5
Transmission efficiency and beam quality of signal combiner with different twist angles.

As shown in Figure 5, the twist angle significantly affects the transmission efficiency and beam quality of the signal combiner. The transmission efficiency fluctuates with increasing twist angle. Between 10° and 70°, the efficiency increases and remains high. Beyond 70°, the efficiency gradually declines, reaching its lowest point at 180°. The beam quality factor M^2 also fluctuates and increases from 10° to 140°, indicating a decline in beam quality. Overall, a twist angle between 10° and 70° maintains both high transmission efficiency and good beam quality.

The twist angle and non-uniform symmetric arrangement distance play significant roles in overall performance. These parameters should be optimized to maintain high transmission efficiency (up to 98.5%) and a minimum M^2 factor (1.06). By carefully balancing these parameters, the design can achieve both high transmission efficiency and excellent beam quality.

4.3 Impact of non-uniform symmetric arrangement on signal combiner

Non-uniform symmetric arrangements of fibers in a signal combiner can significantly affect transmission efficiency and beam quality. When fiber positions and angles are not uniform or symmetric, the light distribution during the combining process becomes uneven, leading to mode mismatch. This results in light scattering and loss, reducing transmission efficiency. Additionally, the inconsistent light path causes mode disturbances, degrading the final beam quality. Therefore, precise fiber arrangement is crucial for efficient light transmission and high beam quality.

This study categorizes non-uniform symmetric arrangements into four scenarios: outward deviation of the middle layer, inward deviation of the middle layer, deviation of multiple fiber cores, and inward deviation of the outermost layer (Figure 6). Each scenario impacts the combiner's performance. Understanding and mitigating these deviations is essential for designing an efficient and high-quality signal combiner.

Based on the optimal parameters of the signal combiner's basic model, an analysis of the transmission efficiency and beam quality under non-uniform symmetric fiber arrangements was conducted. When fibers in the middle layer deviate outward from the central axis, the signal paths become longer, adversely affecting transmission efficiency and beam quality. This outward deviation also results in uneven distances between fibers, further impacting beam synthesis.

Figure 7 illustrates the transmission efficiency and beam quality of the signal combiner for different outward deviation distances of the middle layer.

The outward deviation of the middle layer in a signal combiner affects both transmission efficiency and beam quality. Despite these deviations, the transmission efficiency remains relatively high, indicating effective signal transmission even with some misalignment. As the outward deviation increases from 10 μm to 40 μm, the transmission efficiency improves, peaking at 40 μm. The M^2 factor, which measures beam quality, remains stable across this range, with the best quality observed at 40 μm. This suggests that a 40 μm outward deviation optimizes both transmission efficiency and beam quality.

Figure 7 shows the simulation results for different outward deviations. At 10μm, the transmission efficiency is approximately 96.4% with an M^2 factor of 19.57972. The efficiency peaks at 97.8% at 30 μm before decreasing, while the M^2 factor reaches its minimum value of 18.75102 at 40 μm.

In contrast, inward deviation, where fibers are displaced closer to the central axis, increases fiber interference, especially in compact spaces, affecting beam distribution and uniformity. The impact of different inward deviation distances on transmission efficiency and beam quality is illustrated in Figure 8. Optimizing these deviations is crucial for achieving optimal performance in the signal combiner.

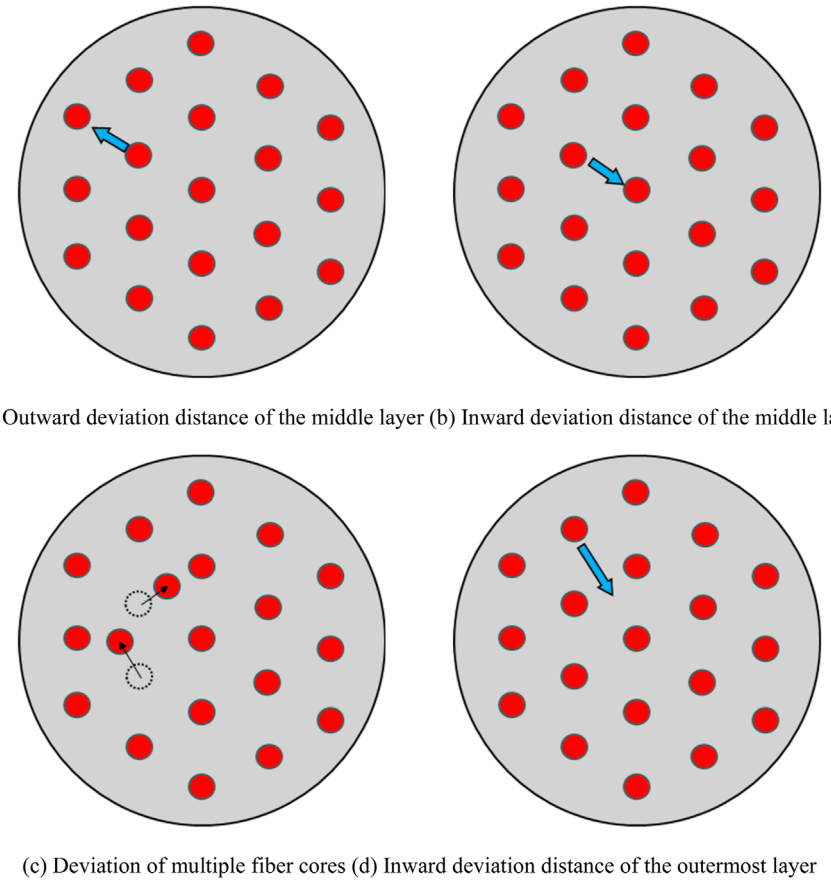

FIGURE 6
Non-uniform symmetric arrangement. **(A)** Outward deviation distance of the middle layer. **(B)** Inward deviation distance of the middle layer. **(C)** Deviation of multiple fiber cores. **(D)** Inward deviation distance of the outermost layer.

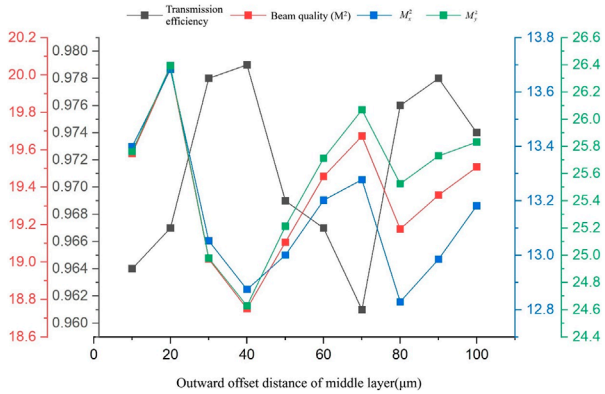

FIGURE 7
Simulation results of outward offset distance of middle layer.

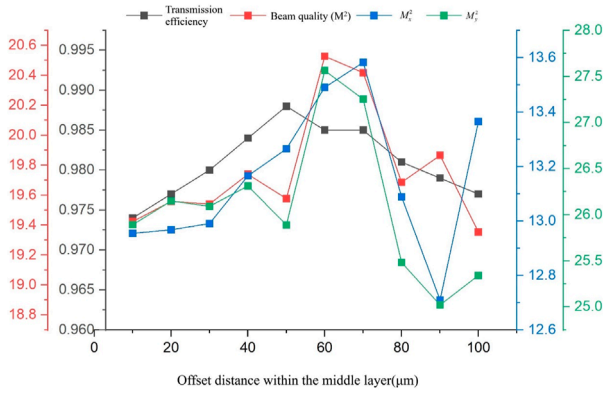

FIGURE 8
Simulation results of offset distance within the middle layer.

According to Figure 8, the transmission efficiency of the signal combiner improves and remains high when the inward offset distance within the middle layer is between 10 and 50 μm. However, beyond 50 μm, the transmission efficiency becomes unstable and significantly drops after 70 μm, indicating that the optimal range for the inward offset is 10–50 μm.

Regarding beam quality, the M^2 factor remains relatively stable for offset distances between 10 and 50 μm. Beyond 50 μm, the

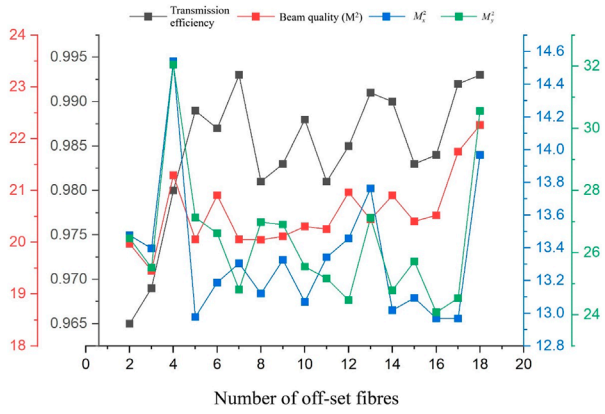

FIGURE 9
Offset fiber root number simulation results.

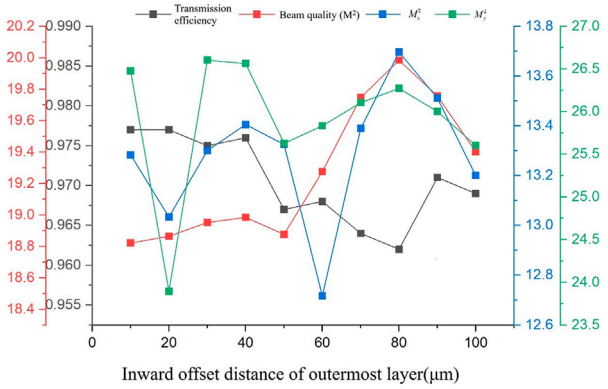

FIGURE 10
Simulation results of inward offset distance of outermost layer.

M^2 factor fluctuates, showing an initial increase followed by a decrease. Therefore, the best overall performance in terms of both transmission efficiency and beam quality is achieved when the offset distance is within 50 μm.

In Figure 8, the simulation results show that at an inward offset of 10μm, the transmission efficiency is 97.4% with an M^2 factor of 19.42289. As the inward offset increases, the transmission efficiency peaks at 98.4% at 40 μm, while the M^2 factor remains stable.

The "number of optical fiber offsets" refers to the number of misaligned fibers in the combiner. Non-uniform arrangements can lead to unstable performance, as misaligned fibers can weaken or distort signals. Figure 9 illustrates the impact of different numbers of offset fibers on transmission efficiency and beam quality, highlighting the importance of minimizing such offsets for optimal combiner performance.

From Figure 9, it is evident that as the number of offset fibers increases, the transmission efficiency of the signal combiner remains high, indicating that the combiner can effectively transmit light signals even with more misaligned fibers. However, the beam quality factor M^2 shows a noticeable upward trend, suggesting that the beam quality degrades as the number of offset fibers increases. The values of M_x^2 and M_y^2 also change, indicating that the beam spreads in both the x and y directions. This means that while the combiner can handle an increased number of offset fibers and maintain good transmission efficiency, the beam quality suffers.

Figure 9 presents the simulation results for the number of offset fibers, illustrating how the number and respective offsets of these fibers impact the overall performance. For instance, at a specific number of offset fibers, the transmission efficiency and beam quality exhibit distinct patterns. The interaction and interference between fibers play a critical role in the system's performance. As the number of offset fibers increases, the potential for signal degradation and mode disturbances also rises, leading to reduced transmission efficiency and beam quality.

When the outermost fibers are offset inward, closer to the central axis, they may become too close to the intermediate or inner-layer fibers. This proximity increases fiber interaction and interference, potentially degrading signal transmission and the overall combining effect. Figure 10 shows the transmission efficiency and beam quality of the signal combiner under different inward offset distances of the outermost fibers, highlighting the trade-off between maintaining high transmission efficiency and ensuring good beam quality.

From Figure 10, it is evident that as the outward offset distance of the outermost layer increases, the transmission efficiency of the signal combiner fluctuates. When the outward offset is within 0–40 μm, the transmission efficiency remains stable and high. However, beyond 50 μm, the transmission efficiency gradually decreases. Additionally, the beam quality factor M^2 shows a decreasing trend as the outward offset increases, indicating a negative impact on beam quality. The effect on beam quality varies in the x and y directions due to changes in symmetry and propagation characteristics.

In Figure 10, which illustrates the simulation results for the inward offset distance of the outermost layer, the data points show that at an inward offset of 10 μm, the transmission efficiency is 97.7% with an M^2 factor of 18.82093. As the offset increases, the transmission efficiency decreases to 96.7% at 50 μm, while the M^2 factor remains relatively stable at 18.87649.

Figures 7–10 highlight the impact of different fiber configurations, including twist angles and non-uniform symmetric alignments, on the signal combiner's performance. For middle layer fibers, an outward deviation between 10 and 40 μm enhances transmission efficiency, peaking at 40 μm, while maintaining stable beam quality. In contrast, increasing the outward offset of the outermost layer fibers beyond 40 μm reduces transmission efficiency and degrades beam quality by disrupting symmetry and propagation properties.

These findings indicate that moderate deviations can optimize transmission paths and reduce interference, but excessive offsets disrupt the necessary symmetry for efficient signal combination and beam integrity. The impact on beam quality is directionally dependent, with variations in both the x and y-axes. Therefore, optimizing the balance between fiber twist angles (optimal around 60°–75°) and controlled non-uniform symmetric alignment (within 10–30 μm spacing) is crucial for maintaining high transmission efficiency and beam quality.

TABLE 1 Transmission efficiency and beam quality of signal combiner at different distances.

Distance	Intermediate layer outward offset		Intermediate layer inward offset		Outermost layer inward offset	
	Transmission efficiency	Beam quality M^2	Transmission efficiency	Beam quality M^2	Transmission efficiency	Beam quality M^2
10 μm	0.964	19.57972	0.974	19.42289	0.977	18.82093
20 μm	0.967	20.03795	0.977	19.55759	0.977	18.86408
30 μm	0.978	19.01574	0.98	19.54035	0.975	18.95194
40 μm	0.979	18.75102	0.984	19.73862	0.976	18.98422
50 μm	0.969	19.10606	0.988	19.57701	0.967	18.87649
60 μm	0.967	19.45702	0.985	20.52663	0.968	19.27507
70 μm	0.961	19.67324	0.985	20.41706	0.964	19.74733
80 μm	0.976	19.17693	0.981	19.68502	0.962	19.98432
90 μm	0.978	19.35747	0.979	19.86497	0.971	19.75594
100 μm	0.974	19.50702	0.977	19.35282	0.969	19.40132

In summary, the interplay between fiber twist and non-uniform arrangement spacing significantly affects the performance of the signal combiner. Adhering to the identified parameter ranges ensures peak efficiency and high beam quality, underscoring the importance of meticulous design considerations in achieving optimal laser system integration.

Table 1 summarizes the key observations, comparing the transmission efficiency and beam quality under different outward and inward offset distances of the intermediate and outermost layers.

From Table 1, the signal combiner's performance varies significantly under different offset distance conditions. For the intermediate layer (both outward and inward offsets) and the outermost layer inward offset, when the offset distance ranges from 10 μm to 50 μm, the transmission efficiency generally remains high, above 97%, indicating effective signal transfer. Within this range, the beam quality (M^2 value) also stays low, suggesting minimal impact on beam uniformity and focusing, resulting in high beam quality.

This indicates that under non-uniform symmetrical offset conditions within 50 μm, the signal combiner can achieve both efficient transmission and superior beam quality, demonstrating excellent optical performance. Therefore, an offset distance range of 10 μm–50 μm is an ideal choice for maintaining the optimal performance of the signal combiner.

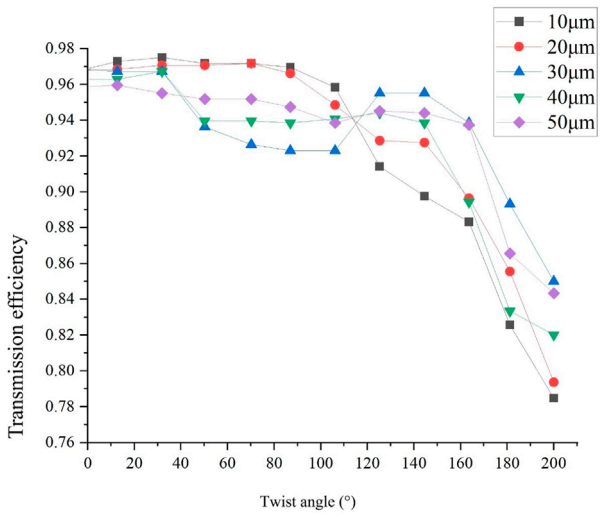

FIGURE 11
Effect of torsion angle and non-uniform symmetric alignment distance on transmission efficiency.

4.4 Comprehensive influence of torsion angle and non-uniform symmetrical arrangement

To find the optimal combination of torsion angle and non-uniform symmetrical arrangement, based on the previous analysis, the influence of different torsion angles on the transmission efficiency of the signal combiner was analyzed under different non-uniform symmetrical arrangement offset distances (10 μm, 20 μm, 30 μm, 40 μm, 50 μm), as shown in Figure 11.

From Figure 11, it is evident that as the torsion angle increases, the transmission efficiency of the signal combiner initially rises, peaking around 60° and 75°, and then decreases. This suggests an optimal range of torsion angles for high transmission efficiency. When considering both torsion angle and non-uniform symmetrical arrangement offset distance, the best transmission efficiency is

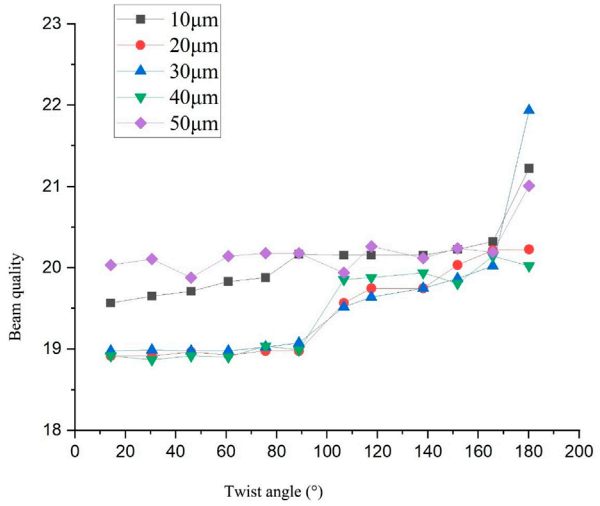

FIGURE 12
Effect of twist angle and non-uniform symmetric alignment distance on beam quality M^2.

achieved when the offset distance is between 10 μm and 30 μm, and the torsion angle is between 15° and 75°. However, if the offset distance increases to 50 μm, the high-efficiency torsion angle range narrows to 15°–45°.

This interaction between torsion angle and offset distance shows that a suitable torsion angle can mitigate the decrease in transmission efficiency caused by non-uniform fiber arrangements. Specifically, when the torsion angle is within 60° and the offset distance is between 10 μm and 30μm, the signal combiner achieves optimal transmission efficiency, consistently above 98%.

Further analysis of the impact of torsion angle and non-uniform symmetrical arrangement on beam quality (M^2) is provided in Figure 12.

From Figure 12, it is evident that as the non-uniform symmetric arrangement distance increases, the M^2 value, which indicates beam quality, also increases. Specifically, when the arrangement distance is between 40 μm and 50 μm, the M^2 value rises significantly, showing a decrease in beam quality and increased beam divergence or inconsistency. In contrast, when the arrangement distance is between 10 μm and 30 μm, and the twist angle is between 10° and 90°, the M^2 value remains lower, indicating better beam quality. Twist angles beyond 105° lead to a significant increase in the M^2 value, further degrading beam quality.

In summary, to achieve high transmission efficiency and good beam quality, the optimal conditions for the signal combiner are a twist angle not exceeding 60° and a non-uniform symmetric arrangement distance between 10 μm and 30 μm. These parameters are guided by adiabatic taper conditions and brightness conservation principles. Adiabatic tapering ensures stable light mode propagation during the fiber tapering process, avoiding mode disturbances from rapid or uneven size changes. The brightness conservation principle maintains constant optical power through the fiber, even with structural changes.

By limiting the twist angle to within 60°, the design avoids mutual interference and mode mismatch caused by excessive distortion, ensuring efficient signal transmission and excellent beam quality. Keeping the non-uniform symmetric arrangement distance between 10 μm and 30 μm balances effective coupling and combining of light waves while reducing cross-interference between fibers. This optimized spacing, combined with adiabatic tapering and brightness conservation, achieves high-efficiency and stable light transmission, maintaining beam quality and consistency.

Currently, this design is validated through software simulations and has not yet been implemented in practical use. Further testing and validation are needed for its future application.

While this study provides valuable insights into the optimization of 19 × 1 fiber signal combiners, it is important to note several limitations. The findings, which indicate that a twist angle not exceeding 60° and a non-uniform symmetric arrangement distance between 10 and 30 μm can achieve high transmission efficiency (up to 98.5%) and good beam quality (minimum M^2 factor of 1.06), are based on theoretical modeling and simulations. These results have not been validated through experimental data or practical tests, which would significantly enhance the credibility and applicability of the research.

To address these limitations, future work should include experimental validation. This would involve fabricating prototypes and conducting performance evaluations using high-precision optical instruments. By comparing simulated and experimental data, the validity of the model can be confirmed, and any discrepancies can guide further refinements. Rigorous testing will validate the design's feasibility in real-world applications and support the development of advanced high-power fiber laser systems.

5 Discussion

This study investigates the impact of fiber twist angle and non-uniform symmetric arrangement on the performance of 19 × 1 fiber signal combiners. The findings reveal that maintaining a twist angle not exceeding 60° and a non-uniform symmetric arrangement distance between 10 and 30 μm under adiabatic tapering and brightness conservation principles can achieve high transmission efficiency and better beam quality. These results provide novel insights into the optimal design parameters for fiber signal combiners, contributing to the advancement of high-power fiber laser systems. The practical implications of these findings are significant, as they offer a robust solution to the limitations of current designs and pave the way for more efficient and reliable laser systems.

To further build on these findings, future research should focus on several key areas. First, experimental validation of the simulation results is essential. This would involve fabricating prototypes and conducting performance evaluations using high-precision optical instruments. By comparing simulated and experimental data, the validity of the model can be confirmed, and any discrepancies can guide further refinements. Second, exploring different types of fiber materials, such as those with varying refractive indices or specialized coatings, could provide additional insights into how material properties affect the performance of the combiner. Third, investigating alternative structural designs, such as incorporating micro-structured or photonic crystal fibers, may offer new opportunities for further improving transmission efficiency and beam quality. Finally, the integration of these optimized combiners

into real-world applications, including industrial, medical, and military uses, will be crucial for demonstrating their practical value and driving the development of advanced high-power fiber laser systems.

6 Conclusion

This study investigates the impact of fiber twist angle and non-uniform symmetric arrangement on the performance of a 19 × 1 fiber signal combiner. The findings reveal that the twist angle and non-uniform symmetric arrangement significantly influence transmission efficiency and beam quality. Specifically, a twist angle not exceeding 60° and a non-uniform symmetric arrangement distance between 10 and 30 μm under adiabatic tapering and brightness conservation principles maintain high transmission efficiency and better beam quality. These results provide novel insights into the optimal design parameters for fiber signal combiners, contributing to the advancement of high-power fiber laser systems and offering practical guidance for enhancing their performance and reliability in various applications.

Data availability statement

The original contributions presented in the study are included in the article/supplementary material, further inquiries can be directed to the corresponding author.

Author contributions

YY: Data curation, Investigation, Methodology, Supervision, Validation, Writing–original draft, Writing–review and editing. TG: Formal Analysis, Resources, Validation, Visualization, Writing–original draft, Writing–review and editing. GL: Conceptualization, Investigation, Software, Writing–original draft, Writing–review and editing. CX: Conceptualization, Investigation, Writing–original draft, Writing–review and editing. ZW: Project administration, Writing–original draft, Writing–review and editing.

Funding

The author(s) declare that no financial support was received for the research, authorship, and/or publication of this article.

Acknowledgments

The authors would like to show sincere thanks to those techniques who have contributed to this research.

Conflict of interest

The authors declare that the research was conducted in the absence of any commercial or financial relationships that could be construed as a potential conflict of interest.

Publisher's note

All claims expressed in this article are solely those of the authors and do not necessarily represent those of their affiliated organizations, or those of the publisher, the editors and the reviewers. Any product that may be evaluated in this article, or claim that may be made by its manufacturer, is not guaranteed or endorsed by the publisher.

References

1. Li X, Huang X, Hu X, Guo X, Han Y. Recent progress on mid-infrared pulsed fiber lasers and the applications. *Opt and Laser Technology* (2023) 158:108898. doi:10.1016/j.optlastec.2022.108898

2. Ahmed SA, Mohsin M, Ali SMZ. Survey and technological analysis of laser and its defense applications. *Defence Technology* (2021) 17(2):583–92. doi:10.1016/j.dt.2020.02.012

3. Richardson DJ, Nilsson J, Clarkson WA. High power fiber lasers: current status and future perspectives [Invited]. *JOSA B* (2010) 27(11):B63–B92. doi:10.1364/josab.27.000b63

4. Hansryd J, Andrekson PA, Westlund M, Li J, Hedekvist PO. Fiber-based optical parametric amplifiers and their applications. *IEEE J Selected Top Quan Electronics* (2002) 8(3):506–20. doi:10.1109/jstqe.2002.1016354

5. Koška P, Baravets Y, Peterka P, Bohata J, Písařík M. Mode-field adapter for tapered-fiber-bundle signal and pump combiners. *Appl Opt* (2015) 54(4):751–6. doi:10.1364/ao.54.000751

6. Brida D, Krauss G, Sell A, Leitenstorfer A. Ultrabroadband Er: fiber lasers. *Laser and Photon Rev* (2014) 8(3):409–28. doi:10.1002/lpor.201300194

7. Pan Z, Yu C, Willner AE. Optical performance monitoring for the next generation optical communication networks. *Opt Fiber Technology* (2010) 16(1):20–45. doi:10.1016/j.yofte.2009.09.007

8. Zhang W, Lang X, Liu X, Li G, Singh R, Zhang B, et al. Advances in tapered optical fiber sensor structures: from conventional to novel and emerging. *Biosensors* (2023) 13(6):644. doi:10.3390/bios13060644

9. Klenke A, Jauregui C, Steinkopff A, Aleshire C, Limpert J. High-power multicore fiber laser systems. *Prog Quan Electronics* (2022) 84:100412. doi:10.1016/j.pquantelec.2022.100412

10. Pal B. Fabrication and modeling of fused biconical tapered fiber couplers. *Fiber integrated Opt* (2003) 22(2):97–117. doi:10.1080/01468030390111922

11. He C, Xiao X, Xu Y, Xiao Y, Zhang H, Guo H. Numerical and experimental investigations on the propagation property of a mid-infrared 7 × 1 multimode fiber combiner. *Opt Express* (2023) 31(13):22113–26. doi:10.1364/oe.491674

12. Fathi H, Närhi M, Gumenyuk R. Towards ultimate high-power scaling: coherent beam combining of fiber lasers. *Photonics* (2021) 8(12):566. doi:10.3390/photonics8120566

13. Gu Y, Lei C, Yang H, Xiao H, Leng J, Chen Z. High-beam-quality signal and pump combiner with large-mode-area fiber for high-power fiber laser and amplifier. *Appl Opt* (2019) 58(6):1336–40. doi:10.1364/ao.58.001336

14. Sibellas A, Adrien J, Durville D, Maire E. Experimental study of the fiber orientations in single and multi-ply continuous filament yarns. *The J The Textile Inst* (2020) 111(5):646–59. doi:10.1080/00405000.2019.1659471

15. Giorgio I, Ciallella A, Scerrato D. A study about the impact of the topological arrangement of fibers on fiber-reinforced composites: some guidelines aiming at the development of new ultra-stiff and ultra-soft metamaterials. *Int J Sol Structures* (2020) 203:73–83. doi:10.1016/j.ijsolstr.2020.07.016

16. Min F, Zhixian L, Zefeng W, Zilun C, Xiaojun X. Research on a 4 × 1 fiber signal combiner with high beam quality at a power level of 12kW. *Opt Express* (2021) 29(17):26658–68. doi:10.1364/oe.433047

17. Feit MD, Fleck Jr JA. Calculation of dispersion in graded-index multimode fibers by a propagating-beam method. *Appl Opt* (1979) 18(16):2843–51. doi:10.1364/ao.18.002843

18. Han JM. *A new interoperability framework for data-driven building performance simulation*. Harvard University (2022). Doctoral dissertation.

19. Koshiba M, Tsuji Y, Hikari M. Time-domain beam propagation method and its application to photonic crystal circuits. *J lightwave Technol* (2000) 18(1):102–10. doi:10.1109/50.818913

20. Saitoh K, Koshiba M. Full-vectorial imaginary-distance beam propagation method based on a finite element scheme: application to photonic crystal fibers. *IEEE J Quan Electronics* (2002) 38(7):927–33. doi:10.1109/jqe.2002.1017609

21. Elsharkawi AS, Tsai IC, Lin XT, Chang CY, Lo YL. Bessel beam propagation using radial beam propagation method at different propagation scales. *Opt Express* (2024) 32(17):30242–55. doi:10.1364/oe.530908

22. Sun J, Liu L, Han L, Zhu Q, Shen X, Yang K. 100 kW ultra high power fiber laser. *Opt Continuum* (2022) 1(9):1932–8. doi:10.1364/optcon.465836

23. Schmidt B, Schaefer M. Advanced industrial laser systems and applications. In: *High-power laser materials processing: applications, diagnostics, and systems VII*, 10525. SPIE (2018).1052502

24. Lipatov DS, Lobanov AS, Guryanov AN, Umnikov AA, Abramov AN, Khudyakov MM, et al. Fabrication and characterization of Er/Yb co-doped fluorophosphosilicate glass core optical fibers. *Fibers* (2021) 9(3):15. doi:10.3390/fib9030015

25. Li B, Zhou JF, Wang Y, Bai Yang 白. 10 kW矩形光斑激光空间合束器光学透镜的有限元热分析. *Acta Photonica Sinica* (2022) 51(2):0251213. doi:10.3788/gzxb20225102.0251213

26. Brockmüller E, Kleihaus L, Wellmann F, Lachmayer R, Neumann J, Kracht D (2022). Highly efficient side-fused signal pump combiners based on CO2-laser restructured optical fibers. In *EPJ Web of Conferences* (Vol. 267, p. 02008). doi:10.1051/epjconf/202226702008

27. Zhou Y, Qiu Q, Yang A, Yang G, Xu Y, Gu Z, et al. All-fiber cascaded combiners for high-power adjustable-ring mode laser beam with a flattop central beam. *Opt and Laser Technology* (2023) 163:109324. doi:10.1016/j.optlastec.2023.109324

28. Liu Y, Huang S, Wu W, Xie L, Zhang C, Li H, et al. 5-kW-level bi-directional high-efficiency pump and signal combiner with negligible beam quality degradation. *IEEE Photon J* (2022) 14(1):1–6. doi:10.1109/jphot.2021.3140004

29. Wu W, Chen Z, Wang Z, Chen J. Beam combining of fiber lasers by a 3× 1 signal combiner at a power> 13 kW. *Opt Fiber Technology* (2020) 54:102109. doi:10.1016/j.yofte.2019.102109

30. Choi IS, Park J, Jeong H, Kim JW, Jeon MY, Seo HS. Fabrication of 4 × 1 signal combiner for high-power lasers using hydrofluoric acid. *Opt Express* (2018) 26(23):30667–77. doi:10.1364/oe.26.030667

31. Yao W, Shen C, Shao Z, Wang J, Wang F, Zhao Y, et al. 790 W incoherent beam combination of a Tm-doped fiber laser at 1941 nm using a 3 × 1 signal combiner. *Appl Opt* (2018) 57(20):5574–7. doi:10.1364/ao.57.005574

32. Zhou X, Chen Z, Wang Z, Hou J, Xu X. High power incoherent beam combining of fiber lasers based on a 7× 1 all-fiber signal combiner. *Opt Eng* (2016) 55(5):056103. doi:10.1117/1.oe.55.5.056103

33. Xu J, Zhou P, Liu W, Leng J, Xiao H, Ma P, et al. Exploration in performance scaling and new application avenues of superfluorescent fiber source. *IEEE J Selected Top Quan Electronics* (2017) 24(3):1–10. doi:10.1109/jstqe.2017.2725838

34. Liu Y, Liu K, Yang Y, Liu M, He B, Zhou J. High power pump and signal combiner for backward pumping structure with two different fused fiber bundle designs by means of pretapered pump fibers. *Opt Express* (2021) 29(9):13344–58. doi:10.1364/oe.422549

35. Jackson SD, Jain RK. Fiber-based sources of coherent MIR radiation: key advances and future prospects (invited). *Opt express* (2020) 28(21):30964–1019. doi:10.1364/oe.400003

36. Alexander VV, Kulkarni OP, Kumar M, Xia C, Islam MN, Terry Jr FL, et al. Modulation instability initiated high power all-fiber supercontinuum lasers and their applications. *Opt Fiber Technology* (2012) 18(5):349–74. doi:10.1016/j.yofte.2012.07.014

37. Linslal CL, Ayyaswamy P, Maji S, Sooraj MS, Dixit A, Venkitesh D, et al. Challenges in coherent beam combining of high power fiber amplifiers: a review. *ISSS J Micro Smart Syst* (2022) 11(1):277–93. doi:10.1007/s41683-022-00099-4

38. Dong L, Samson B. *Fiber lasers: basics, technology, and applications*. Amsterdam: CRC Press (2016).

39. Arumugam AB, Selvaraj R, Subramani M, Vemuluri RB. Damping and instability characteristics of uniform and non-uniform composite multifunctional semi-active sandwich structures under rotating environment. *Composites Sci Technology* (2022) 219:109203. doi:10.1016/j.compscitech.2021.109203

40. Zhao Z, Chen H, Zhang Z, Li J, Zhu F, Wan W, et al. High peak power femtosecond cylindrical vector beams generation in a chirped-pulse amplification laser system. *Chin Opt Lett* (2022) 20(3):031405. doi:10.3788/col202220.031405

41. Ye G, Yuan T, Zhang Y, Wang T, Zhang X. Recent progress on laser interferometry based on vortex beams: status, challenges, and perspectives. *Opt Lasers Eng* (2024) 172:107871. doi:10.1016/j.optlaseng.2023.107871

42. Zervas MN, Codemard CA. High power fiber lasers: a review. *IEEE J selected Top Quan Electronics* (2014) 20(5):219–41. doi:10.1109/jstqe.2014.2321279